Supporting Information available

Table S1.

The results of the fit by two Lorentzian functions to the C=C stretching vibration of DFBH. The weak shoulder peak in the lower frequency side of the C=C mode around 1636 cm^{-1} are omitted from the Table. ν_P and $\Delta\nu$ represent the peak position and the bandwidth (full width at half maximum) of each vibrational mode. The unit of frequency and bandwidth is cm^{-1}. ρ_r is the reduced density of the solvent scaled by the critical density of the solvent.

T (K)	P (MPa)	ρ_r	ν_P(C=C)	$\Delta\nu$(C=C)
298	0.1	2.86	1653.5	9.8
298	30.0	2.94	1652.7	8.9
350	30.0	2.80	1651.5	10.0
450	30.0	2.43	1649.5	11.8
520	30.0	2.11	1647.4	14.2
520	10.0	1.72	1647.6	13.5

Table S2.

The results of the fit by Lorentzian functions to the C=C stretching vibration and the C=O stretching vibration of BP. The values of the weak shoulder peak in the lower frequency side of the C=C mode around 1580 cm^{-1} are omitted from the Table. *AN* is calculated by Eq. (1).

T (K)	P (MPa)	ρ_r	ν_P(C=C)	$\Delta\nu$(C=C)	ν_P(C=O)$_1$	$\Delta\nu$(C=O)$_1$	ν_P(C=O)$_2$	$\Delta\nu$(C=O)$_2$	*AN*
298	0.1	2.86	1599.1	7.0	1652.9	12.1	1665.5	8.3	32.6
298	30.0	2.94	1598.7	7.4	1651.9	13.2	1664.7	8.7	35.0
350	30.0	2.80	1598.3	7.9	1654.3	14.8	1665.5	9.0	29.2
450	30.0	2.43	1597.8	9.6	1659.2	16.1	1666.9	10.7	17.4
520	30.0	2.11	1595.3	12.0	1660.6	16.1	1666.8	9.3	14.0
520	10.0	1.72	1595.8	12.1	1662.4	15.5	1668.6	9.4	9.5

Table S3.

The results of the fit by Lorentzian functions to the C=C stretching vibration and the C=O stretching vibration of DFBP.　The values of the weak shoulder peak in the lower frequency side of the C=C mode around 1636 cm^{-1} are omitted from the Table.

| T (K)	P (MPa)	ρ_r	ν_P(C=C)	$\Delta\nu$(C=C)	ν_P(C=O)$_1$	$\Delta\nu$(C=O)$_1$	ν_P(C=O)$_2$	$\Delta\nu$(C=O)$_2$
298	0.1	2.86	1650.0	8.2	1690.0	14.9	1704.9	16.4
298	30.0	2.94	1649.2	8.5	1688.3	14.8	1703.4	18.8
350	30.0	2.80	1648.3	9.3	1688.5	16.5	1703.0	18.3
450	30.0	2.43	1646.2	11.4	1689.4	18.7	1702.5	18.9
520	30.0	2.11	1644.3	12.6	1690.3	20.5	1702.6	18.1
520	10.0	1.72	1644.2	13.2	1691.1	21.0	1703.6	17.1

Table S4.

Results of the fitting of the experimental Raman spectrum around C-O region of 2-propanol at different thermodynamic condition by a sum of Lorentzian functions.

| T (K)	P (MPa)	ρ_r	ν_P(C-O)	$\Delta\nu$(C-O)	ν_P(C-H)$_1$	$\Delta\nu$(C-H)$_1$	ν_P(C-H)$_2$	$\Delta\nu$(C-H)$_2$
298	0.1	2.86	953.4	12.4	918	10.6	935	16.0
298	30.0	2.94	953.1	12.4	918	12.6	935	16.0
350	30.0	2.80	951.6	15.2	918	14.8	935.6	21.4
450	30.0	2.43	947.3	30			929.8	36.1
520	30.0	2.11	944.3	44.6			917.3	19.6
520	10.0	1.72	944.8	48.8			917.7	17.6

Figure S1

A schematic drawing of the experimental system for the time-resolved resonance Raman measurement for the high-temperature and high-pressure solution.
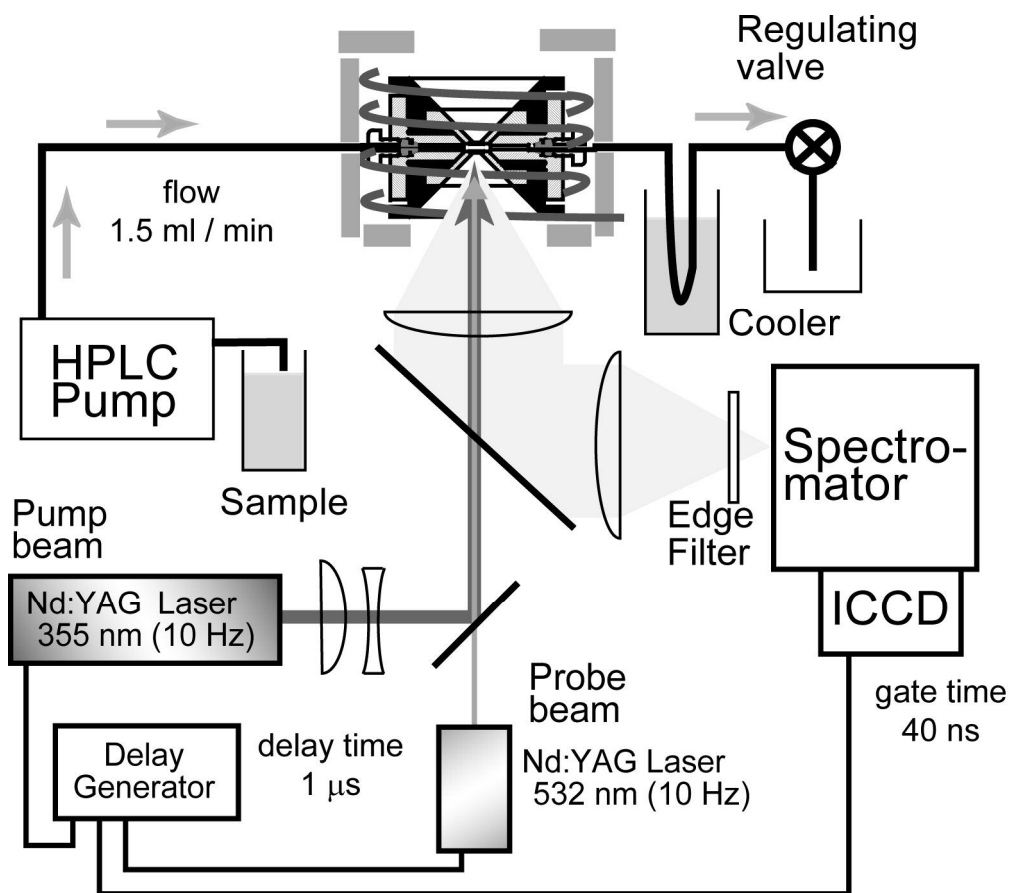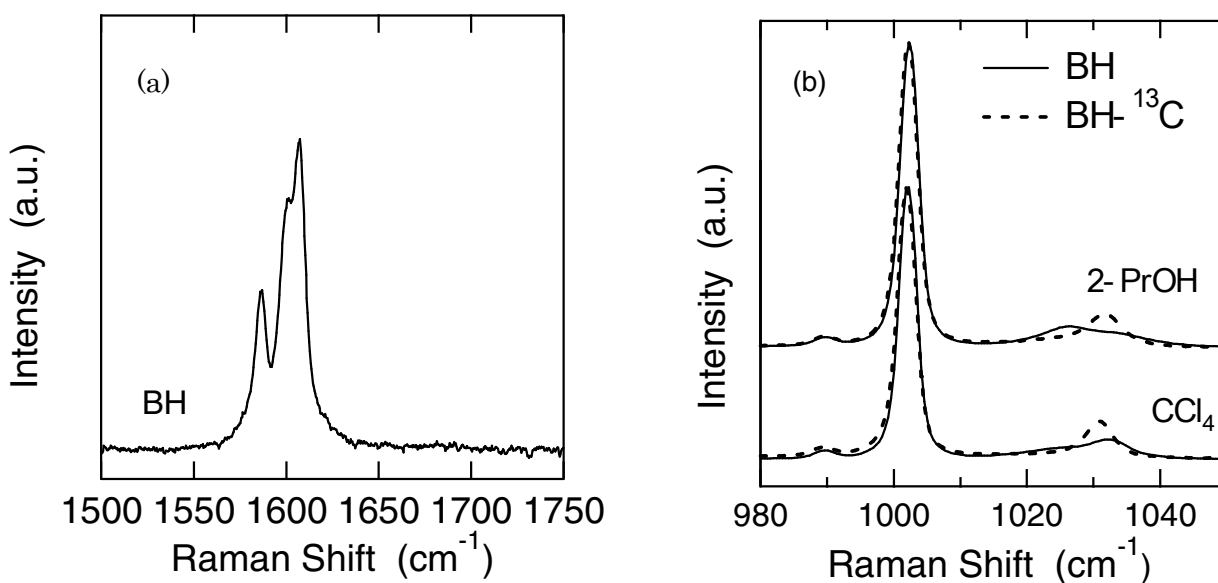
Figure S2

Transient absorption spectra of the DFBP/2-propanol solution after the excitation by the 266 nm pulse at 29.4 MPa and 520 K.   Transient absorption measurement was performed in a collinear alignment of a pump pulse and a probe beam.   As the probe beam, a xenon lamp (Eagle technology, XC-150SRE) was used.   Before the sample cell, an IR-cut filter was placed.   After the sample cell, the probe beam was collimated to the optical fiber and transferred to the spectromator equipped with an ICCD camera (the same system as is used for the time-resolved Raman).   Before the entrance of the fiber, an UV-cutoff filter was placed in order to remove the pump light.   The gate width was fixed to 1 μs.   The high pressure optical cell designed for the absorption spectrum measurements was used.   The details are described elsewhere (Amita, F.; Okada, K.; Oka, H.; Kajimoto, O, *Rev. Sci. Instrum.* **2001**, *72*, 3605).   The concentration of the sample solution was ca. 1 mM.   At the higher temperature of 520 K, the absorption spectrum due to DFBPK became rather broader than those observed at 298 K (Shoute L. C. T.; Mittal, J. P., *J. Phys. Chem.* **1993**, *97*, 8630), while the peak position did not shift so much.   Comparing the spectrum at 10 μs after the excitation with that at 500 ns, there is no significant difference in the spectrum shapes, suggesting that the hydrogen-abstraction reaction proceeds within 500 ns.
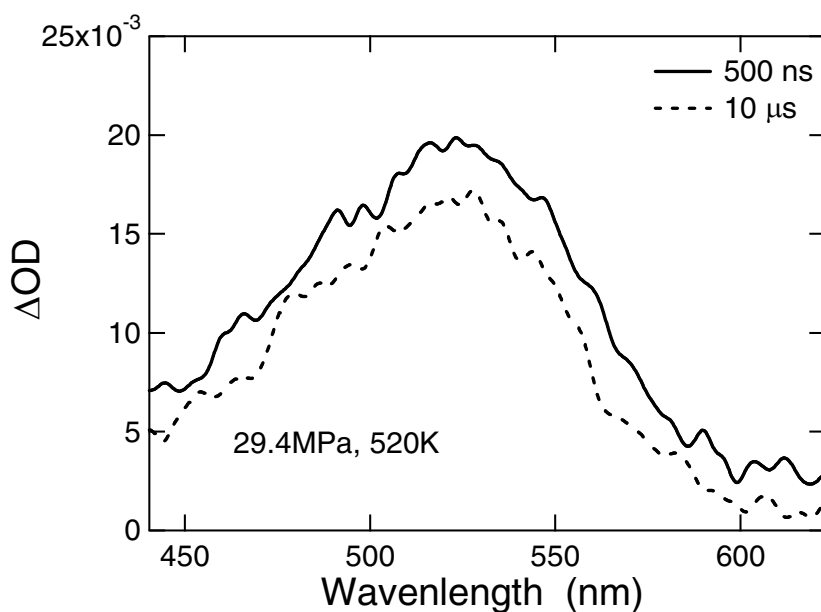
Figure S3

(a) Raman spectra of BH around the frequency region of the C=C stretching mode in 2-PrOH. There are multiple bands around 1600 cm^{-1}, while the corresponding band of DFBH is simpler (around 1650 cm^{-1}).　　(b) Raman spectra of BH (solid lines) and BH-^{13}C (broken limes) around the frequency region of the C-O stretching mode in carbon tetrachloride and 2-propanol.　Beside the very strong band assigned to the ph-12 mode of the phenyl ring, there appear weak bands around 1026 cm^{-1} and 1034 cm^{-1} in 2-PrOH.　On the other hand, only a single Raman band is observed around 1031 cm^{-1} for BH-^{13}C.　According to the DFT calculations, the vibrational mode with the C-O stretching character of BH is expected to appear as split bands due to the coupling between ν(C-O) and ν(ph-18) (1059 cm^{-1} and 1045 cm^{-1}).　On the other hand, in the case of BH-^{13}C, such a split disappears due to the lower frequency shift of the C-O stretching mode (1028 cm^{-1} from the DFT calculation), which is consistent with the experimental observation.　The C-O stretching mode of BH-^{13}C is considered to be hidden behind the strong ph-12 mode.

Figure S4

The bandwidths for (a) the C=C stretching modes and (b) the C=O or C-O stretching mode at different densities (temperatures), respectively. For simplicity, only the one vibrational mode is plotted in the case of splitting bands; for the C=C stretching mode of other molecules, the main large modes are plotted; for the C=O stretching modes of BP and DFBP, the lower frequency bands (band 1, see Fig. 5) are plotted;